

Advanced Models for Predicting Aggregate Rutting Behavior

H. Ceylan & A. Guclu

Department of Civil, Construction and Environmental Engineering, Iowa State University of Science and Technology, Ames, Iowa, USA

E. Tutumluer & O. Pekcan

Department of Civil and Environmental Engineering, University of Illinois, Urbana, Illinois, USA

ABSTRACT: Artificial neural network (ANN) based advanced aggregate rutting models have been developed and compared for performance using laboratory test data. The primary goal has been to properly characterize the loading stress path dependent permanent deformation behavior from advanced repeated load triaxial tests that can simulate in the laboratory the varying stress states under actual moving wheel load conditions. The aggregate specimens tested were the Federal Aviation Administration (FAA) specified P209 base and P154 subbase materials also used in the pavement test sections of the FAA's National Airport Pavement Test Facility (NAPTF). Due to the complex loading regimes followed in the laboratory tests and the full-scale NAPTF testing, the ANN rutting models that altogether considered as inputs the static and dynamic components of the applied stresses and the loading stress path slope produced the greatest accuracy. Such advanced neural network models can better describe the aggregate rutting behavior under actual field loading conditions.

KEY WORDS: Artificial neural networks, unbound aggregates, rutting, permanent deformation modeling, laboratory stress path testing

1 INTRODUCTION

Rutting is the repeated load-induced permanent deformation of a flexible pavement. For pavement geomaterials, typically unbound base/subbase and subgrade soil, rutting is the only failure mechanism of relevance as no bound layers are involved. The subgrade soils in low to medium volume roads and thick granular layers in airport flexible pavements are more prone to rutting. Depending on the large magnitude and moving nature of wheel loads and the relative strength of the pavement layers, a significant portion of the total permanent deformations can occur in pavement geomaterials.

Recent field studies have indicated that actual traffic loading when applied to pavement test sections resulted in significantly higher permanent deformations in the base and subgrade layers when compared to rutting occurred due to the similar magnitude and amount of loads applied in repeated plate loading (Brown and Brodrick, 1999; Hornych et al., 2000). With rutting distress being the main performance indicator and cause of failure in pavement geomaterial layers, it is of utmost importance to consider the effects of moving wheel loads and stress rotations on the pavement rutting performances.

Permanent deformation behavior of airport pavement granular base/subbase layers is currently being studied at the Federal Aviation Administration's (FAA's) Center of Excellence (COE) for Airport Pavement Technology established at the University of Illinois. To account for the rutting performances of especially thick granular layers, a comprehensive set of repeated load triaxial tests were conducted in the laboratory using an advanced triaxial test apparatus named UI-FastCell (Tutumluer and Seyhan, 1999). The experimental program included both constant and variable confining pressure type triaxial tests to account for heavy wheel loads and variations of the static and dynamic stress states causing continuous extension and compression type loading regimes on a pavement element under a moving aircraft wheel. The granular specimens tested are the FAA specified P209 base and P154 subbase materials also used in the pavement test sections of the FAA's National Airport Pavement Test Facility or NAPTF (Garg, 2003).

This paper presents the latest research findings on the development of artificial neural network (ANN) based unbound aggregate permanent deformation models from the laboratory test data. The primary goal is to properly model the accumulation of permanent deformations in laboratory specimens as a function of the repeated load applications and the loading stress path dependent stress states that are used to simulate in the laboratory the actual moving wheel load field effects. The developed ANN models consider the most proper combinations of input variables accounting for the various static and dynamic stress states and the loading stress path slopes. The performances of the ANN rutting models are compared to those of the conventional ones having "a priori" functional forms.

2 LABORATORY TESTING NEEDS FOR PERMANENT DEFORMATION

An evaluation of permanent deformation in the laboratory should consider varying the number of load repetitions, applied stress states, and applied shear stress ratios as a minimum. In triaxial conditions, the specimen permanent deformations can be adequately obtained from the test data when both the mean pressure $p = (\sigma_1 + 2\sigma_3)/3$ and the deviator (shear) stress $q = (\sigma_1 - \sigma_3)$ are included in the material characterization. The effects of stress path loading and principal stress rotations under moving wheels are also important to investigate in the laboratory for a better and more comprehensive understanding of the complex permanent deformation behavior.

In the constant confining pressure (CCP) tests, it is only possible to apply one constant stress path ($\Delta q/\Delta p = 3$) representing those stress states that occur directly under the wheel loading. The applied stress ratio (σ_1/σ_3 or total vertical to horizontal stress) at which the CCP test is performed in the laboratory affects the accumulation of permanent deformation. Considering field conditions, stress ratios higher than 6 are often encountered in a granular pavement layer at the centerline loading. To realistically simulate stress states in the field, a proper test procedure for determining rutting potential of an aggregate material should consider such high ratios in laboratory testing.

The pavement in the field is usually loaded by moving wheel loads, which at any time impose varying magnitudes of vertical, horizontal, and shear stresses in the aggregate layer accompanied by the rotation of the principal stresses. This type of dynamic loading can be ideally simulated in the laboratory by the variable confining pressure (VCP) type repeated load triaxial tests. In the VCP tests, the stress path slope ($m = \Delta q/\Delta p$) varies generally from the -1.5 extension state extreme to the $m=3$ CCP condition to offer the capability to apply a wide combination of stress paths by pulsing both cell pressure, σ_3 , and vertical deviator stress, σ_d . Such stress path loading tests better simulate actual field conditions since in the pavement structure the confining stresses acting on the material are also cyclic in nature. Typically,

some radial distance away from the centerline of loading, the horizontal component of the dynamic wheel load can become greater in magnitude than the vertical component. In that case, an extension type of loading can be more critical on top of the base. Such a variety of stress paths may cause different loading effects on pavement elements, which are not yet fully studied and understood to explain permanent deformation accumulation.

3 MATERIALS TESTING

The FAA specified granular base and subbase materials P209 and P154, both crushed aggregate, were selected for permanent deformation testing using the advanced repeated load triaxial test device University of Illinois-FastCell. The P209 base material is classified as A-1-a according to AASHTO procedure and as GP-GM according to ASTM procedure whereas the P154 subbase aggregate is classified as A-1-b according to AASHTO procedure and as SW-SM according to ASTM procedure. For the P209 and P154 unbound aggregate materials, 7.5 mm and 1.7 mm are the average sizes, D_{50} , 19 mm and 37 mm are the top sizes, and 8% and 12% are the percentages passing No. 200 sieve size (0.075 mm), respectively.

3.1 Advanced Laboratory Test Program

A total of 4 stress path tests were conducted on the crushed aggregate P209 and P154 samples for the selected constant stress path slopes. These are one CCP ($m = 3$) stress path and 3 VCP stress path slopes, $m = 1.5, 0, -1$, of the stress path-testing program that the specimens were subjected to at four different confining or hydrostatic pressures $\sigma_3 = \sigma_s$. Table 1 lists the stress states applied on the specimens for evaluating the effects of applied stress states and stress path loadings on the permanent deformation accumulation. A total of 52 tests were carried out on each of the P154 and P209 aggregates for the combined CCP and VCP test program. After the overall static confining pressure $\sigma_3 = \sigma_s$ was applied on the specimen, permanent deformation testing was conducted by: (i) pulsing only in the vertical (σ_{1d}) direction for the CCP ($m = 3$) compression test, and (ii) pulsing both in the vertical (σ_{1d}) and radial (σ_{3d}) directions for the VCP1 ($m = 1.5$), VCP2 ($m = 0$), and VCP3 ($m = -1$) compression and extension tests (see Table 1).

3.2 Permanent Deformation Model Development

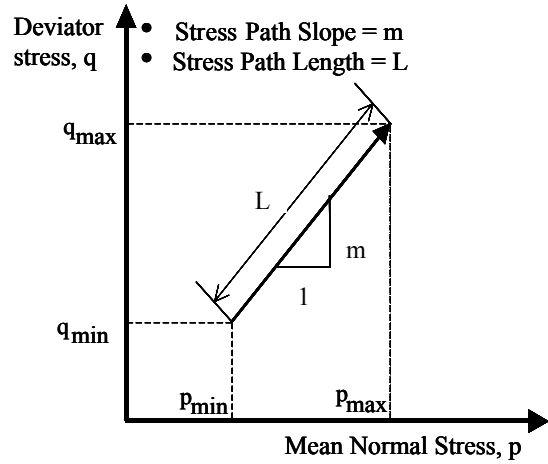
Based on the experimental data obtained from the laboratory test program, seven different models, accounting for static confining pressure (σ_s), dynamic stresses in both axial (σ_{1d}) and radial (σ_{3d}) directions, stress path length (L), stress path slope (m), and number of load applications (N), shown in Table 2, were studied and the model performances were compared to predict the axial permanent strain (ϵ_p) behavior of the P209 and P154 base/subbase materials. Due to the complex loading regimes followed especially in VCP testing, models had to be analyzed simultaneously using the static and dynamic components of the applied stresses. While models 1 to 5 (see Table 2) can only be applied to individual test data for predicting permanent strain accumulation with number of load applications, models 6 and 7 can use the complete database from all the CCP and VCP tests with the stress path slope m included as an additional variable with values ranging from -1 to 3. Even for the cases of not considered horizontal pulsing only ($m = -1.5$) and pure shear loading ($\Delta p = 0$) with a vertical slope ($m = \infty$), models 6 and 7 can predict permanent strain accumulation with the term in the parenthesis varying from 32.6 to 1 for $m = -1.5$ to ∞ .

Table 1: Selected stress states and laboratory testing program for the P209/P154 aggregates

Constant Confining Pressure (CCP) Tests			Variable Confining Pressure (VCP) Tests								
Stress Path Slope m = 3 (Compression states)			Stress Path Slope m = 1.5 (Compression states)			Stress Path Slope m = 0			Stress Path Slope m = -1 (Extension states)		
$\sigma_3 = \sigma_s$ (kPa)	σ_{1d} (kPa)	σ_{3d} (kPa)	$\sigma_3 = \sigma_s$ (kPa)	σ_{1d} (kPa)	σ_{3d} (kPa)	$\sigma_3 = \sigma_s$ (kPa)	σ_{1d} (kPa)	σ_{3d} (kPa)	$\sigma_3 = \sigma_s$ (kPa)	σ_{1d} (kPa)	σ_{3d} (kPa)
20.7	62.1	0	20.7	72.73	18.15	20.7	65.55	65.55	20.7	15.46	61.82
20.7	103.5	0	20.7	120.9	30.22	20.7	109.0	109.0	20.7	25.67	102.8
20.7	114.9	0	20.7	169.1	42.30	20.7	152.4	152.4	20.7	35.95	143.8
20.7	186.3	0	20.7	218.1	54.51	20.7	196.6	196.6	20.7	46.37	185.4
34.5	103.5	0	34.5	120.9	30.22	34.5	109.0	109.0	34.5	25.67	102.8
34.5	172.5	0	34.5	202.1	50.51	34.5	182.1	182.1	34.5	42.92	171.7
34.5	241.5	0	34.5	282.4	70.59	34.5	254.6	254.6	34.5	60.03	240.0
34.5	310.5	0	34.5	362.8	90.74	34.5	327.0	327.0	34.5	77.07	308.3
55.2	165.6	0	55.2	193.6	48.44	55.2	174.5	174.5	55.2	41.12	164.5
55.2	276.0	0	55.2	323.0	80.73	55.2	291.1	291.1	55.2	68.66	274.5
55.2	386.4	0	55.2	451.6	112.8	55.2	407.1	407.1	55.2	95.98	383.8
69.0	207.0	0	69.0	241.9	60.44	69.0	218.0	218.0	69.0	51.41	205.5
69.0	345.0	0	69.0	403.4	100.8	69.0	363.6	363.6	69.0	85.70	342.8

Table 2: Permanent strain models studied for the FAA NAPTF base/subbase aggregates

Model 1	$\epsilon_p = a \cdot \sigma_s^b \cdot N^c$
Model 2	$\epsilon_p = a \cdot \sigma_s^b \cdot \sigma_{1d}^c \cdot N^d$
Model 3	$\epsilon_p = a \cdot \sigma_s^b \cdot \sigma_{3d}^c \cdot N^d$
Model 4	$\epsilon_p = a \cdot \sigma_s^b \cdot \sigma_{1d}^c \cdot \sigma_{3d}^d \cdot N^e$
Model 5	$\epsilon_p = a \cdot \sigma_s^b \cdot L^c \cdot N^d$
Model 6	$\epsilon_p = a \cdot \sigma_s^b \cdot N^c \cdot \left(1 + \frac{1}{10^m}\right)^d$
Model 7	$\epsilon_p = a \cdot \sigma_s^b \cdot L^c \cdot N^d \cdot \left(1 + \frac{1}{10^m}\right)^e$
a, b, c, d, and e : regression parameters	



All models were applied to 5 different testing data sets. Four of them had stress path slopes, -1, 0, 1.5, and 3, respectively, and the fifth data set contained all four data sets combined. Table 3 lists the regression correlation coefficients (R^2 s) achieved from using these five data sets. The R^2 values for $m = -1$ were in general the lowest possibly due to the high noise and fluctuations in the recorded triaxial data. The best model performances were obtained for the $m = 3$ CCP tests resulting in the highest R^2 values. In general, model 4, accounting for both static and dynamic stresses in both axial and radial directions, showed better correlations than those achieved from other models employing only single dynamic stress (either axial or radial dynamic stress) or no dynamic stress for both P209 and P154 materials. Rather low regression correlation values (R^2 s), around 0.5, were also obtained for

the intermediate stress path slopes, $m = -1$ and 1.5 . Nevertheless, models 6 and 7, which properly account for the various static and dynamic stress states and stress path loading conditions, gave relatively higher R^2 's on all data. This result is indeed a very promising finding in that such models can predict granular material permanent deformation accumulation with satisfactory performance using approximate stress states applied in the granular layer and whether or not these stresses are due to a stationary loading or moving wheel loading with stress rotations.

The use of the permanent strain models, given in Tables 2 and 3, developed from the laboratory test results require validation and calibration with actual field rut measurements. Such field data on the performances of the P209/P154 granular layers are currently available from the FAA's NAPTF flexible pavement test sections. Current ongoing research efforts are focused on the validation and calibration activities using the NAPTF field data (Hayhoe and Garg, 2002).

Table 3: Correlation coefficients (R^2 values) indicating permanent strain model performances

Model No.	R^2 Values for All data	R^2 Values for Stress Path Slope (m)			
		$m = -1$	$m = 0$	$m = 1.5$	$m = 3$
P209 FAA Base Material					
1	0.02	0.17	0.11	0.16	0.12
2	0.56	0.24	0.70	0.47	0.86
3	0.41	0.42	0.72	0.32	-
4	0.80	0.38	0.78	0.53	-
5	0.05	0.41	0.71	0.50	0.84
6	0.73	-	-	-	-
7	0.86	-	-	-	-
P154 FAA Subbase Material					
1	0.02	0.05	0.35	0.03	0.04
2	0.46	0.62	0.53	0.32	0.78
3	0.16	0.44	0.52	0.34	-
4	0.60	0.62	0.53	0.35	-
5	0.02	0.42	0.53	0.32	0.79
6	0.60	-	-	-	-
7	0.65	-	-	-	-

4 NEURAL NETWORK MODELING OF PERMANENT DEFORMATION BEHAVIOR

A total of seven ANN based permanent deformation prediction models, which account for the overall static confining pressure ($\sigma_3 = \sigma_s$), dynamic stresses in both axial (σ_{1d}) and radial (σ_{3d}) directions, stress path slope (m), and number of load applications (N), shown below, were studied and the models were compared for performance in predicting the output, laboratory measured axial permanent strains (ϵ_p) of the P209 and P154 base/subbase aggregate specimens. The input parameters of the ANN models are listed below:

ANN Model 1: σ_s , m, and N

ANN Model 2: σ_s , σ_{3d} , and N

ANN Model 3: σ_s , σ_{3d} , m, and N

ANN Model 4: σ_s , σ_{1d} , and N

ANN Model 5: σ_s , σ_{1d} , m, and N

ANN Model 6: σ_s , σ_{3d} , σ_{1d} , and N

ANN Model 7: σ_s , σ_{3d} , σ_{1d} , m, and N

4.1 Backpropagation Artificial Neural Networks

Backpropagation type ANN models were trained in this study using the experimental test results for predicting the permanent deformations of the P209 base and P154 subbase materials. An independent testing data set was used to check the prediction performances of the different ANN models. Backpropagation ANNs are very powerful and versatile networks that can be taught a mapping from one data space to another using the examples of the mapping to be learned. The term “backpropagation network” actually refers to a multilayered, feed-forward neural network trained using an error backpropagation algorithm. The learning process performed by this algorithm is called “backpropagation learning,” which is mainly an error minimization technique (Haykin, 1999; Hecht-Nielsen, 1990; Parker, 1985, Rumelhart et al., 1986; & Werbos, 1974).

As with many ANNs, the connection weights in the backpropagation ANNs are initially selected at random. Inputs from the mapping examples are propagated forward through each layer of the network to emerge as outputs. The errors between those outputs and the correct answers are then propagated backwards through the network and the connection weights are individually adjusted to reduce the error. After many examples (training patterns) have been propagated through the network many times, the mapping function is learned with some specified error tolerance. This is called supervised learning because the network has to be shown the correct answers for it to learn. Backpropagation networks excel at data modeling with their superior function approximation capabilities (Haykin, 1999; Meier and Tutumluer, 1998).

4.2 Neural Network Design and Training

To train the backpropagation type neural networks with the laboratory test results for P154 and P209 subbase and base materials, a set of network architectures was required. Varying number of input parameters (σ_s , σ_{3d} , σ_{1d} , m and N) constituted the network input layers. The only output variable for each network was the axial permanent strain (ϵ_p). Based on the available test results, ANN training data files were formed comprising of 8,774 rows of data for the P154 aggregate and 10,994 rows of data for the higher quality P209 material with varying number of input parameters and the single output response of ϵ_p . A randomly selected set of 500 test results were reserved as an independent testing data set for both materials to confirm the proper training and to validate the performance of the trained ANN models. After trying several network architectures, a network with two hidden layers was exclusively chosen for the ANN models trained in this study. Satisfactory results were obtained in the previous studies with these types of networks due to their ability to better facilitate the nonlinear functional mapping (Ceylan, 2002).

To train the ANN models, first the entire training data sets were randomly shuffled and normalized and then divided into training and testing data sets. The number of input parameters ranged from 3 to 5 in these data sets. 8,224 and 10,494 rows of data were used in the training data sets for P154 and P209 materials, respectively, to train seven different network architectures for each material type. The remaining 500 data patterns for each material were used then for testing to verify the prediction ability of each trained ANN model.

Since ANNs learn relations and approximate functional mapping limited by the extent of the training data, the best use of the trained ANN models were achieved in interpolation.

Each training epoch of the network consisted of one pass over the entire training data sets. The testing data sets were used to monitor the training progress. Overall, the MSEs decreased as the networks grew in size with increasing number of input parameters in the input layer. Figure 1 depicts for the laboratory data the training progress curves obtained from ANN models 1 and 7 for the network architectures having two hidden layers with 15 nodes in each layer. After around 2,000 learning cycles, the mean squared error (MSE) values leveled off for the training and testing sets of both models and adding more nodes to the hidden layers did not help further reduce the MSEs. Figure 1 clearly shows that the more sophisticated the models get (models with 4-5 input parameters), the lower MSE values were obtained when compared to the simpler models (models with 2 input parameters). The very close MSE values obtained from the training and testing sets for models 7 for both P209 base and P154 subbase materials (see Figure 1) is also a very good indication of proper network training, in other words, the trained networks actually learned the nonlinear relationship between the input parameters and the output variable (ϵ_p) for the given data sets.

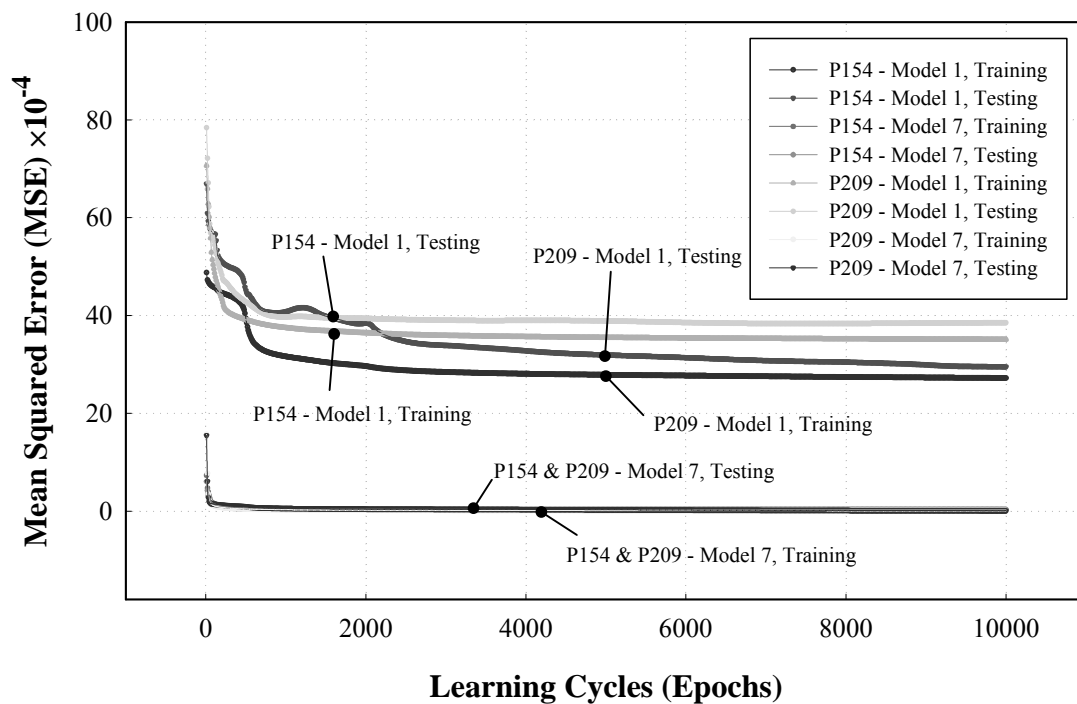


Figure 1: Training progress curves for ANN models 1 and 7 for P154 and P209 materials

4.3 Performance of Trained ANN Models

The prediction performance of ANN models 1 and 7 trained using the laboratory test results are depicted in Figure 2. As can be clearly seen in Figure 2, permanent strain (ϵ_p) predictions from model 7 are much closer to the line of equality than the predictions from model 1. For P154 subbase material, the average absolute error (AAE) for the 500 testing data set for model 7 is 3.1% while the corresponding AAE value for model 1 is 8.5%. The AAE values obtained for models 7 and 1 for P209 base material are 3.4% and 14.5%, respectively.

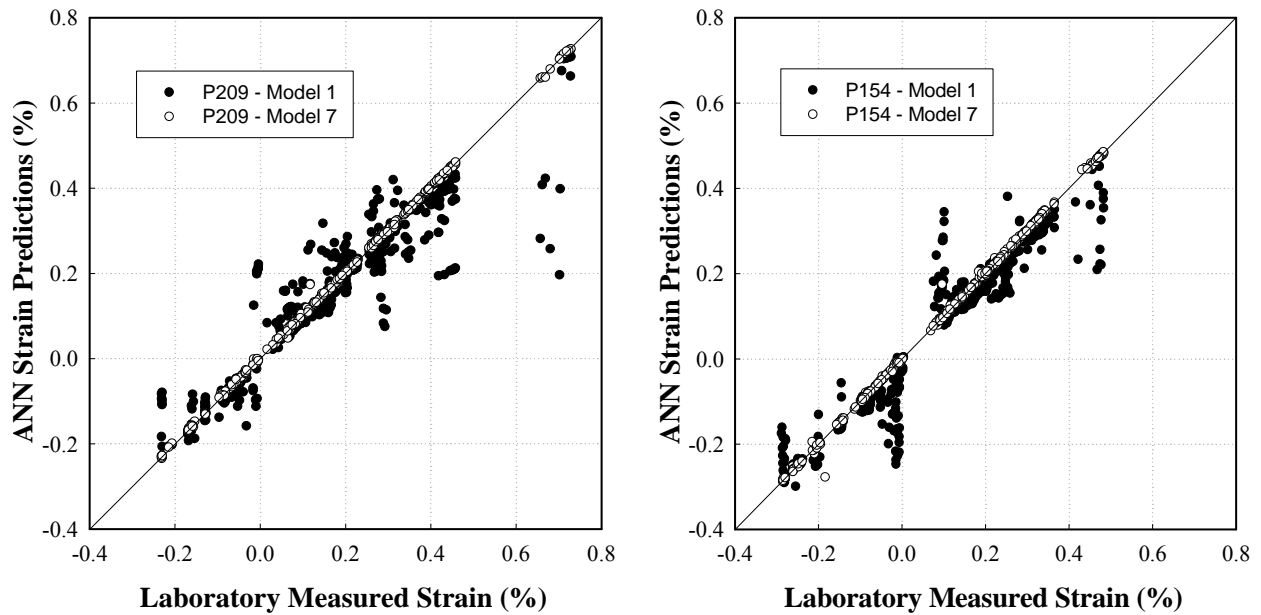


Figure 2: Predicted and measured axial permanent strains for P154 and P209 materials

Figure 3 shows the training MSE values of the seven ANN models trained in this study using the experimental test results. In all of the ANN trainings, very low values of MSEs were consistently obtained for the more sophisticated ANN models, i.e., models 4-7. When all the input parameters (σ_3 , σ_{3d} , σ_{1d} , m and N) were included in ANN models, the ability of predicting the permanent strain values has improved dramatically. Accordingly, ANN models 6 and 7 produced the lowest MSEs, i.e., the best predictions of the permanent strain values for both material types. The inclusion of stress path slope (m) in model 7 did not improve the results much when compared to model 6 results. This can be explained with the fact that ANN model 6 could capture in its connections the various stress path slopes m , which is a dependent variable of σ_{3d} , and σ_{1d} and can be expressed as a function of the stress states using the dynamic components of the bulk and shear stresses. But, as reported by Tutumluer et al. (2001) if information about m is missing, prediction ability of the models for base and subbase materials will be dramatically reduced since changing the applied principal stress ratio has significant effect on the directional dependency of the granular material deformation characteristics. The better prediction performances of the ANN models 4-7 can be explained with the main observation that all of these more advanced models include the axial/vertical dynamic stresses (σ_{1d}) as an input parameter. This shows that axial permanent strain behavior is highly influenced by the applied axial/vertical dynamic stress (σ_{1d}) and the aggregate material's overall applied stress states.

5 SUMMARY/CONCLUSIONS

A modeling study has been undertaken to develop artificial neural network (ANN) models for predicting the rutting or permanent deformation behavior of the Federal Aviation Administration's (FAA's) P209 base and P154 subbase courses constructed and tested at the National Airport Pavement Test Facility (NAPTF). The primary goal has been to properly model the loading stress path dependent permanent deformation behavior from advanced repeated load triaxial tests that can simulate in the laboratory the actual moving wheel load

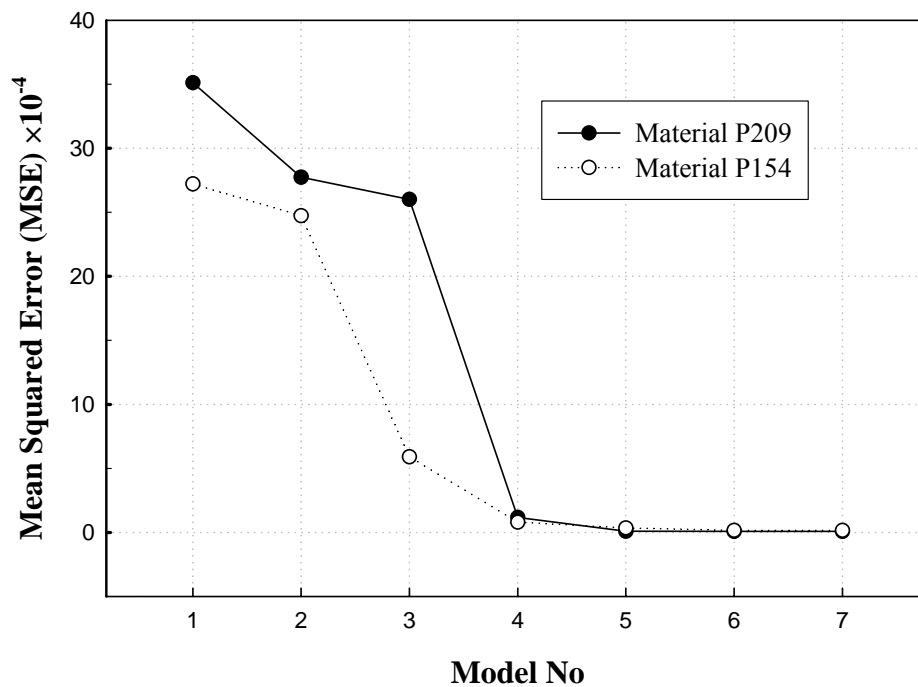


Figure 3: Comparison of the MSE values for different ANN models and material types

conditions. The ANN models were developed using the permanent strain data produced by a comprehensive laboratory testing program in which tests were conducted to apply various stress path loadings on the granular material specimens using the advanced repeated load triaxial test device University of Illinois-FastCell. Due to the complex loading regimes followed in the laboratory tests, ANN models that analyzed simultaneously the static and dynamic components of the applied mean and shear stresses produced significantly better predictions. As expected, ANN-based models outperformed the regression-based models, which are usually limited to assignment of “a priori” best-fit power functions. Such advanced ANN models better describe the rutting behavior of granular materials under actual field loading conditions and should be more commonly used in geomaterials characterization.

6 REFERENCES

- Brown, S.F. and Brodrick, B.V., 1999. *25 Years' Experience with the Pilot-Scale Nottingham Pavement Test Facility*. Proceedings of the International Conference on Accelerated Pavement Testing, Reno, Nevada, October 18-20.
- Ceylan, H., 2002. *Analysis and Design of Concrete Pavement Systems Using Artificial Neural Networks*. Ph.D. Dissertation, University of Illinois at Urbana-Champaign, Urbana, IL.
- Garg, N., 2003. *Permanent Deformation Behavior of the Granular Layers Tested at the National Airport Pavement Test Facility*. Presented at the 82nd Annual Transportation Research Board Meeting, Washington, D.C., January (<http://www.airtech.tc.faa.gov/NAPTF/Download/>).
- Hayhoe, G.F. and Garg, N., 2002. *Subgrade Strains Measured In Full-Scale Traffic Tests With Four- and Six-Wheel Landing Gears*. Proceedings of the FAA Airport Technology Transfer Conference, Atlantic City, NJ, May 5-8 (<http://www.airtech.tc.faa.gov/NAPTF/Download/>).

- Haykin, S. 1999. *Neural Networks: A Comprehensive Foundation*. Prentice-Hall, Inc., New Jersey.
- Hecht-Nielsen, R. 1990. *Neurocomputing*. Addison-Wesley, New York.
- Hornych, P, Kazai, A., and Quibel, A., 2000. *Modeling A Full-Scale Experiment of Two Flexible Pavement Structures With Unbound Granular Bases*. In *Unbound Aggregates in Road Construction*, Edited by A.R. Dawson, A.A. Balkema Publishers, Proceedings of the 5th Unbound Aggregates in Roads (UNBAR5) Symposium, University of Nottingham, U.K., June 21-23, pp. 359-367.
- Meier, R. and Tutumluer, E. 1998. *Uses of Artificial Neural Networks in the Mechanistic-Empirical Design of Flexible Pavements*. Proc. Intl. Workshop on Artificial Intelligence and Mathematical Methods in Pavement and Geomechanical Engineering Systems. Florida International University, Florida, 1-12.
- Parker, D.B. 1985. *Learning Logic*. Technical Report TR-47, Center for Computational Research in Economics and Management Science, Massachusetts Institute of Technology, Cambridge, MA.
- Rumelhart D.E., Hinton, G.E. and Williams, R.J., 1986. *Learning Representations by Back-Propagating Errors*. *Nature*, 323: 533-536.
- Tutumluer, E., Ceylan, H., and Seyhan, Ü., 2001. *Advanced Characterization of Granular Material Behavior Using Artificial Neural Networks*. XVth International Conference on Soil Mechanics and Geotechnical Engineering, Istanbul, Turkey, August 27-31, 2001.
- Tutumluer, E. and Seyhan, Ü., 1999. *Laboratory Determination of Anisotropic Aggregate Resilient Moduli Using an Innovative Test Device*. In *Transportation Research Record: Journal of the Transportation Research Board*, No. 1687, TRB, National Research Council, Washington, DC, pp. 13-21.
- Werbos, P. 1974. *Beyond Regression: New Tools for Prediction and Analysis in the Behavioral Sciences*. Ph.D. Dissertation, Harvard University, MA.